Letter

Quantum transduction is enhanced by single mode squeezing operators

Changchun Zhong [1,*] Mingrui Xu,[2] Aashish Clerk,[1] Hong X. Tang,[2,3] and Liang Jiang [1,†]

[1]*Pritzker School of Molecular Engineering, University of Chicago, Chicago, Illinois 60637, USA*

[2]*Department of Electrical Engineering, Yale University, New Haven, Connecticut 06520, USA*

[3]*Yale Quantum Institute, Yale University, New Haven, Connecticut 06520, USA*

(Received 8 May 2022; accepted 10 October 2022; published 21 October 2022)

Quantum transduction is an essential ingredient in scaling up distributed quantum architecture and is actively pursued based on various physical platforms. However, demonstrating a transducer with positive quantum capacity is still practically challenging. In this Letter, we discuss a new approach to relax the impedance matching condition to half impedance matching condition, achieved by introducing two-photon drive in the electro-optic transducer. We show the quantum transduction capacity can be enhanced and can be understood in a simple interference picture with the help of the Bloch-Messiah decomposition. The parameter regimes with positive quantum capacity is identified and compared with and without the drive, indicating that the parametric drive-induced enhancement is promising in demonstrating quantum state conversion and is expected to boost the performance of transduction with various physical platforms.

DOI: 10.1103/PhysRevResearch.4.L042013

Introduction. Superconducting qubit based quantum networks—processing quantum information with superconducting circuits [1] and transmitting quantum signals by optical photons [2]—are appealing architectures for future communication systems [3,4]. To scale up such networks, coherent conversion between microwave and optical (MO) states—quantum transduction—is indispensable as superconducting qubits lack intrinsic optical transitions. However, realizing MO quantum states conversion turns out to itself be extremely challenging with current technology [5–8]. Considering the transduction as a quantum channel to obtain a positive quantum channel capacity, the channel must have both high channel transmissivity and low added noise, e.g., at least, 50% transmissivity is needed [9]. Although significant advances have been made recently [10–26], the traditional direct quantum transducer (DQT), which linearly converts MO quantum signals by beam splitter coupling, is still below the threshold where quantum capacity is zero.

A perfect transducer has infinite quantum capacity, which requires even more stringent impedance matching condition [27]. In recent years, respecting the fact that quantum capacity can be enhanced with two-way communication [28,29], there are approaches to use the classical channel [30–34], adaptive control [35,36], multipass interference [37], etc., to overcome the challenge of full impedance matching. Although encouraging, all these schemes require additional classical control, access to other output ports, or even infinitely squeezed input fields.

For future high-bandwidth quantum transduction, it is still desirable to construct a DQT. In this Letter, we discuss a new DQT scheme based on a cavity electro-optic (EO) transducer [38]. By applying a parametric drive to the microwave mode, we find a new approach that can relax the matching condition—two transduction quadratures are impedance matched—to the *half-matching condition*—only one quadrature needs to be matched [27,37]. We show that a generic transducer satisfying the half-matching condition yields an infinite quantum capacity. This capacity can be achieved using solely operations on the transducer's active input and output modes, respecting the channel coding theorem [39]. Note that the utility of half-impedance matched quantum transducers was discussed in Ref. [37] in a different context and without any direct connection to quantum capacity.

In the ideal case with no intrinsic loss and zero detuning, we show the parametric drive enables the half-matching condition that enhances the transduction channel capacity enormously. This observation is appealing especially given the current challenges in transducer design and fabrication to simultaneously achieve near-unity transmissivity and ground-state conversion.

The parametric drive-enabled half-matching condition can also function in a more practical situation with intrinsic noise and finite detuning. In general, the half-matching condition cannot be fully achieved by the drive, and the parametric-amplified noise could severely degrade the channel. Whereas a general approach to maintain the enhancement is yet to find, *in some parameter regime* we show there is a drive-induced exponential increase in the mode coupling strength within the Bogoliubov framework, and a proper noise canceling scheme can be adopted. Note this similar technique has been used in an optomechanical system for solving a practically

*zhong.changchun@uchicago.edu

†liang.jiang@uchicago.edu

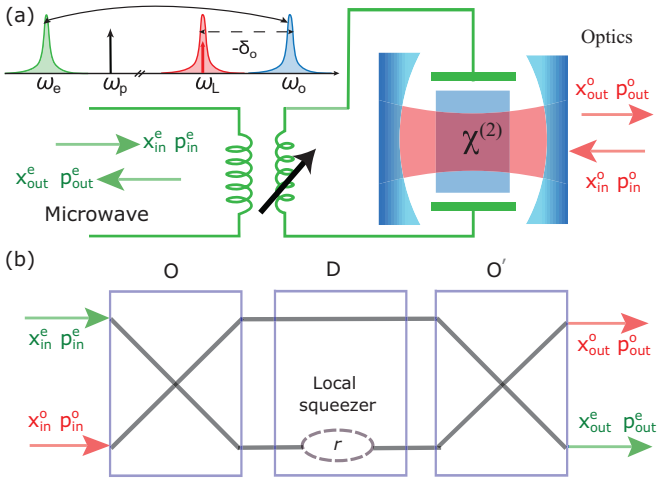

FIG. 1. (a) Schematic for a cavity electro-optic transducer. A laser pump is applied on one of the optical modes (red) and it generates a beam splitter interaction between the optical $\hat{a}$ (blue) and the microwave $\hat{b}$ (green), shown in the spectrum diagram. The microwave mode parametric drive is introduced through the tunable superconducting inductance, indicated by the black arrow. (b) The discrete model of the local squeezer sandwiched by two imperfect transducers, which can be realized by the simple continuous design depicted in (a).

challenging problem, e.g., canceling the counter-rotating term for the side band unresolved system [40], cooling [41], enhancing light-matter interaction [42–46], and nonreciprocity [47].

The parametric drive induces amplified noise to the Bogoliubov mode, degrading the transduction performance. Nevertheless, we observe the capacity still gains from the coupling enhancement in some parameter regime. More interestingly, the amplified noise can be eliminated completely if we implement the noise cancellation technique, e.g., generating squeezed vacuum as the mode reservoir [47,48], thus, the capacity enhancement can be maintained in larger parameter space.

The model. Without losing generality, we take a cavity EO system for demonstration. Cavity EO is a hybrid superconducting-photonic device where a superconducting resonator is integrated with an optical cavity, consisting of material which features Pockels nonlinearity, e.g., AlN. As shown in Fig. 1(a), the electrical field from the resonator can change the material refraction index, which modifies the frequency of optical photons. In reverse, microwave field can be modulated by the cavity optical fields due to the optical *rectification* of Pockels material. With the material nonlinearity and a triple resonant design [22], a three-wave mixing between two chosen optical modes and an electrical resonator can be realized, and by appropriately driving one of the two optical modes with laser frequency ω_L, a beam splitter interaction can be generated $\hbar g(\hat{a}^\dagger\hat{b} + \hat{a}\hat{b}^\dagger)$, where $\hat{a}$ and $\hat{b}$ denote the optical and microwave mode operators, respectively. g is the laser-enhanced coupling strength. With the system on resonance, one can get a transduction channel—a single-mode bosonic loss channel with transmissivity (i.e., determinant of the quadrature-basis transmission matrix) [46,49],

$$\eta = \frac{4C_g}{(1+C_g)^2}\zeta_e\zeta_o, \tag{1}$$

where $C_g \equiv 4g^2/\kappa_o\kappa_e$ is the MO *cooperativity*. We have denoted (κ_o, κ_e) as the (optical, microwave) total dissipation rates and (ζ_o, ζ_e) as the (optical, microwave) extraction ratio [50]. Currently, EO transducer's transmissivity is reported to be around several percent, which is still below the 50% threshold for a general Bosonic loss channel to have positive quantum capacity [38,49].

In this Letter, we consider enhancing the transduction by introducing parametric drive to the superconducting resonator, which can be realized in a superconducting resonator with intrinsic tunable inductance and is commonly used in cavity-based Josephson amplifiers [51]. The total Hamiltonian is given as

$$\hat{H}/\hbar = -\left(\delta_o + \frac{\omega_p}{2}\right)\hat{a}^\dagger\hat{a} + \left(\omega_e - \frac{\omega_p}{2}\right)\hat{b}^\dagger\hat{b} + g(\hat{a}^\dagger\hat{b} + \hat{a}\hat{b}^\dagger) + \nu(e^{-i\theta}\hat{b}^{\dagger 2} + e^{i\theta}\hat{b}^2), \tag{2}$$

where $\delta_o = \omega_L - \omega_o < 0$ is the optical drive detuning. ν, ω_p, and θ are the parametric pump strength, frequency and phase, respectively. Note the Hamiltonian is written in the rotating frame of half of the parametric pump. Quite interestingly, when the system is on resonance, the channel transmissivity becomes [49]

$$\eta_\nu = \frac{4C_g}{(1+C_g)^2 - 4C_\nu}\zeta_e\zeta_o, \tag{3}$$

where we call $C_\nu \equiv 4\nu^2/\kappa_e^2$ as the *squeezing cooperativity*. In this paper, without stating it otherwise, we are interested in the stable regimes when $C_\nu < (1+C_g)^2/4$.

In Fig. 2, we numerically plot the consequences of introducing this drive whereas keeping other parameters ideal, e.g., unit extraction ratios and system on resonance. Figure 2(a) shows the channel transmissivity with different squeezing as a function of the MO cooperativity. The parametric drive, in general, increases the transmissivity, indicating a positive capacity is potentially achievable with smaller C_g, thus, relaxing the demanding matching condition for the experiment. Figure 2(b) gives the quantum capacity lower bound of the transduction channel (see a brief review of quantum channel in the Appendix [49,52]). Indeed, we see that the parametric drive changes the channel behaviors and increases the quantum capacity for all C_g. The shining white curve is determined by

$$C_\nu = \tfrac{1}{4}(1-C_g)^2, \tag{4}$$

and we will show later this curve exactly traces the parameters that make the transducer fulfill the *half-matching condition*, giving the transducer an optimal quantum capacity. Across the line the channel switches between a bosonic loss channel and an amplification channel. Note the system is stable as long as the squeezing is not extremely high, indicated by the yellow dashed line in Fig. 2(b). This squeezing enhanced quantum transduction channel is our first key observation in this Letter.

Euler decomposition of the scattering matrix. A clear physical picture of the enhancement can be obtained by looking

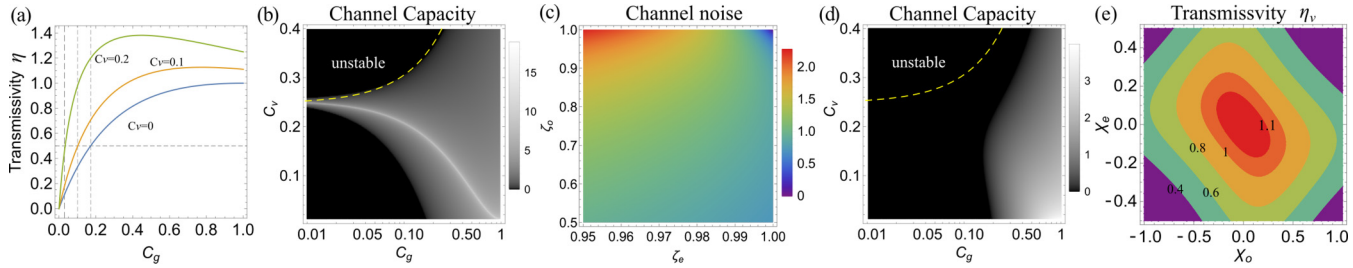

FIG. 2. (a) The channel transmissivity as a function of the MO cooperativity C_g with squeezing cooperativities $C_v = 0, 0.1, 0.2$, respectively. The horizontal dashed lines mark the boundary where the system reaches the positive quantum capacity threshold. The vertical lines help in viewing the corresponding C_g threshold. (b) The quantum capacity lower bound is in terms of C_v and C_g. The eye-catching white line marks the boundary where the channel transmissivity crosses unity—the system goes from a bosonic loss channel to an amplification channel. In (a) and (b), the extraction ratios are taken to be perfect in order to highlight the key consequences of introducing intracavity squeezing. (c) The channel noise as a function of extraction ratios with $C_g = 0.14$, $C_v = 0.16$. (d) The capacity lower bound as in (b) with extraction ratios $\zeta_o = 0.95$, $\zeta_e = 0.99$. (e) The channel transmissivity with respect to the detuning, with $C_g = 0.4$, $C_v = 0.15$, $\zeta_e = 0.99$, $\zeta_o = 0.95$.

at the scattering matrix structure. For system on-resonance and with unit extraction ratios, the scattering matrix $\mathbf{S}_x$ which connects the input and output mode quadratures $\mathbf{x}_{in} = (\hat{x}^a_{in}, \hat{p}^a_{in}, \hat{x}^b_{in}, \hat{p}^b_{in})^T$, $\mathbf{x}_{out} = (\hat{x}^a_{out}, \hat{p}^a_{out}, \hat{x}^b_{out}, \hat{p}^b_{out})^T$ is given by a 4×4 symplectic matrix [49]. For any symplectic matrix, we can always find a Bloch-Messiah decomposition $\mathbf{S}_x = \mathbf{ODO}'$ [53], where $\mathbf{O}, \mathbf{O}'$ are symplectic orthogonal matrices—characterizing beam splitters and phase shifters—and $\mathbf{D}$ is a diagonal matrix—characterizing squeezing of individual mode (see Ref. [49] for expressions). *Remarkably*, the parameter C_v only appears in the $\mathbf{D}$ matrix, which means the scattering process can be characterized as a local squeezer sandwiched by two C_v-independent transformations as depicted in Fig. 1(b). Such a kind of transduction channel can, in general, be made to satisfy the *half-matching condition* by tuning the squeezer in the middle. To get a flavor of the physics, we write down the quadrature transformation from $\mathbf{S}_x$,

$$\hat{x}^b_{out} = \frac{\sqrt{C_g}(1+r)}{1+C_g}\hat{p}^a_{in} + \frac{r-C_g}{(1+C_g)}\hat{x}^b_{in},$$
$$\hat{p}^b_{out} = -\frac{\sqrt{C_g}(1+1/r)}{1+C_g}\hat{x}^a_{in} + \frac{1/r-C_g}{1+C_g}\hat{p}^b_{in}, \tag{5}$$

where $r = \frac{1+C_g+2\sqrt{C_v}}{1+C_g-2\sqrt{C_v}}$. Obviously, if $r = C_g$ [leading to Eq. (4)], we have $\hat{x}^b_{out} = \sqrt{C_g}\hat{p}^a_{in}$, $\hat{p}^b_{out} = -1/\sqrt{C_g}\hat{x}^a_{in} + (1/C_g - 1)\hat{p}^b_{in}$ where the reflection in $\hat{x}^b_{out}$ quadrature is completely canceled by interference. We, thus, achieved the half-matching condition that one quadrature is reflectionless, and the other quadrature is not. As we show, a transduction channel with the half-matching condition has infinite quantum capacity, which should be called perfect transduction. Releasing the perfect matching condition to the *half-matching condition* as the perfect transduction channel is our another key contribution and will be significantly helpful in future transducer designs [27,37].

Bogoliubov mode and near-amplification threshold transduction. The above discussion captures the major physics with unit extraction ratios. If the extraction ratios are not unity, the system couples to extra source of noise which will be amplified and contaminates the output signal. This would potentially kill the gain from the parametric drive. In general, the channel noise expression has a very complicated dependence on $(C_g, C_v, \zeta_e, \zeta_o)$ and we numerically show it in Fig. 2(c). The channel noise quickly increases as the extraction ratios deviates from one, which severely degrade the quantum capacity as shown in Fig. 2(d). Handling the amplified noise is, thus, essential in maintaining the enhancement. In the following, we show it is indeed possible in some parameter regime.

In practice, besides adding squeezing, we can play with another knob—the system detuning—to change the channel transmissivity [49]. In general, we have

$$\eta_v = \frac{4C_g\zeta_o\zeta_e}{C_g^2 + C_g(2+8\chi_e\chi_o) + (1-4C_v+4\chi_e^2)(1+4\chi_o^2)}, \tag{6}$$

where $\chi_o = \Delta_o/\kappa_o$, $\chi_e = \Delta_e/\kappa_e$, and $\Delta_o \equiv \delta_o + \omega_p/2$, $\Delta_e \equiv \omega_e - \omega_p/2$. As shown in Fig. 2(e), the channel transmissivity decreases as we increase the system detuning, which is within expectation for a less-resonant system. Note reducing η_v can also simply achieved by lowering the squeezing. However, with detuning tunable, we can use the tool of *Bogoliubov* transformation to better understand the enhancement, and noise elimination can be performed such that capacity degradation is mitigated.

Define a Bogoliubov mode $\hat{b}_s$ through the transformation [54,55] $\hat{b}_s = \cosh(r)\hat{b} + e^{-i\theta}\sinh(r)\hat{b}^\dagger$ where the mode dissipation rate $\kappa_s = \kappa_e$ and the parameter r is the *effective squeezing* which satisfies $\tanh(2r) = 2\nu/\Delta_e \equiv \beta$. Obviously, the transformation is valid only with $2\nu < \Delta_e$. We can rewrite the Hamiltonian Eq. (2) in terms of the Bogoliubov mode as

$$\hat{H}_s/\hbar = -\Delta_o\hat{a}^\dagger\hat{a} + \omega_s\hat{b}_s^\dagger\hat{b}_s + g_s(\hat{a}^\dagger\hat{b}_s + \hat{a}\hat{b}_s^\dagger), \tag{7}$$

where $\omega_s = \sqrt{\Delta_e^2 - (2\nu)^2}$ and $\Delta_o < 0$. Equation (7) takes exactly the same form as a beam splitter interaction, except that the coupling strength g is replaced by $g_s = g\cosh(r)$ which can be exponentially enhanced by the effective squeezing. Obviously, the channel transmissivity is obtained as

$$\eta_s = \frac{4C_s}{(1+C_s)^2}\zeta_o\zeta_s, \tag{8}$$

where $C_s = 4g_s^2/\kappa_o\kappa_s$ is the Bogoliubov-optical (BO) mode cooperativity, and ζ_s is the Bogoliubov mode extraction ratio. Note this transmissivity η_s is defined in terms of the Bo-

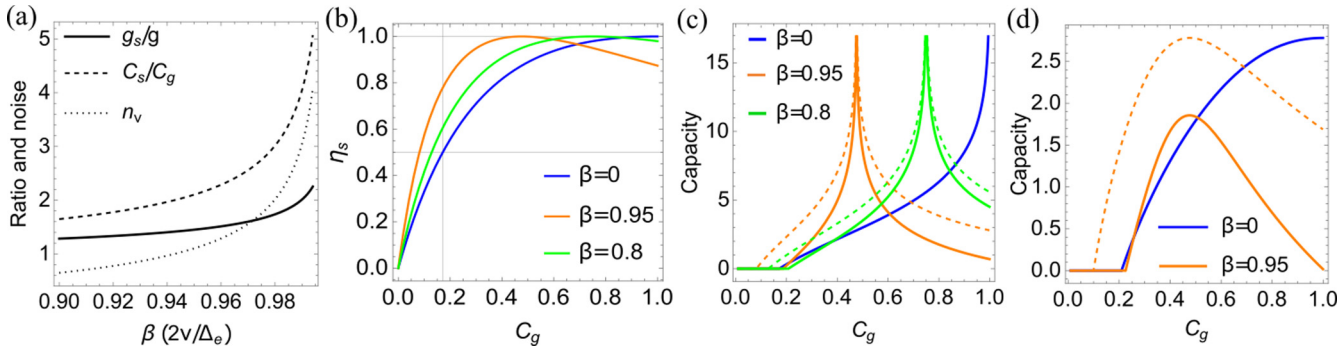

FIG. 3. (a) The coupling strength and cooperativity enhancement, and the squeezing-induced noise in terms of the parameter $\beta = 2\nu/\Delta_e$. (b) and (c) depict the transmissivity η_s and the quantum capacity lower bound as a function of the MO cooperativity with giving $\beta = \{0, 0.8, 0.95\}$, corresponding to the solid blue, green, and orange curves. The solid curves in (c) show the lower bound including squeezing induced noise, and the dashed orange and green lines in (c) show the same bound by assuming the induced noise is eliminated. Extraction ratios are assumed to be one in (b) and (c). (d) The capacity lower bound with respect to C_g for $\beta = \{0, 0.95\}$ and extraction ratios $\zeta_e = 0.97$, $\zeta_o = 0.9$. The orange solid (dashed) includes (excludes) the squeezing induced noises. Note the noise elimination needs an input squeezing that is equal to the squeezing from the parametric drive, which is $10\log_{10} e^{4\nu}$ dB.

goliubov mode which will not be confused with η_ν. Since the BO cooperativity depends on the square of the coupling strength, the channel transmissivity, which depends on the cooperativity, is expected to increase as the coupling strength is enhanced. As shown in Fig. 3(a), the solid and dashed curves depict the exponential enhancement of the coupling strength and cooperativity as the parameter β approaches one, which corresponds to the *amplification threshold* of the system [56]. The change of channel transmissivity η_s is shown in Fig. 3(b) with respect to the MO cooperativity. We see it is possible by adding squeezing to get higher transmissivity even if C_g is small. The orange curve ($\beta = 0.95$) can get to the $\eta_s = 0.5$ threshold with much smaller C_g than the blue curve (no squeezing).

This coupling enhancement comes with a side effect—the squeezing-amplified noise which couples to the Bogoliubov mode. This noise is given by $n_\nu = \cosh(2r)n_{\rm th} + \sinh^2(r)$, where $n_{\rm th}$ is the thermal photon of the microwave bath [49]. In the ideal case, the microwave resonator sits in a very cold environment, and without stating it otherwise we assume it to be vacuum in the numerical evaluations. Still, the noise n_ν is proportional to $\sinh^2(r)$, which could ruin the channel from realizing any quantum conversion as the system gets close to amplification threshold. As shown by the dotted line in Fig. 3(a), the squeezing-amplified noise also increases along with β.

Admittedly, the coupling enhancement and the amplified noise are a pair of competing factors. Fortunately for quantum transduction, we still gain from the transmissivity enhancement in some regime, and we can benefit even more if we adopt the technique of noise elimination [49]. The evidence is given by the quantum channel capacity lower bound as shown in Fig. 3(c) for unit extraction ratios and Fig. 3(d) for $\zeta_e = 0.97$ and $\zeta_o = 0.9$. In Fig. 3(c), the blue curve shows the lower bound for $\beta = 0$. As we increase β, the optimal capacity can be achieved for C_g being smaller as shown by the green and orange solid curves. Moreover, if the technique of noise elimination is adopted [47–49], the capacity gets even bigger, and the positive value spread to larger parameter regime as depicted by the dashed green and orange curves. Figure 3(d) gives the capacity lower bound degraded by the nonunity extraction ratios. Still, larger capacity can be achieved by the parametric drive, and noise cancellation further enhances the transduction channel in broader parameter regimes as shown by the orange solid and dashed curves.

Discussion. A general transducer with the half-matching condition is given by

$$\hat{x}^b_{\rm out} = \xi\hat{x}^a_{\rm in} + \gamma\hat{x}^b_{\rm in}, \quad \hat{x}^a_{\rm out} = \frac{1}{\xi}\hat{x}^b_{\rm in},$$
$$\hat{p}^b_{\rm out} = \frac{1}{\xi}\hat{p}^a_{\rm in} \qquad \hat{p}^a_{\rm out} = \xi\hat{p}^b_{\rm in} - \gamma\hat{p}^a_{\rm in}. \tag{9}$$

Take $a \to b$, for example, one can show perfect transduction can be realized by first squeezing (antisqueezing) the input $\hat{p}^a_{\rm in}$ ($\hat{x}^a_{\rm in}$) then squeezing (antisqueezing) the output $\hat{x}^b_{\rm out}$ ($\hat{p}^b_{\rm out}$) without resorting to any control on other inputs or outputs. Note this differs from the main approach suggested in Ref. [37]. In addition, we point out that the half-matched transducer defines a two-way perfect transduction channel. To achieve that one can do encoding by squeezing the input quadratures ($\hat{x}^b_{\rm in}$, $\hat{p}^a_{\rm in}$) whereas antisqueezing ($\hat{p}^b_{\rm in}$, $\hat{x}^a_{\rm in}$), and perform decoding at the output by squeezing ($\hat{x}^b_{\rm out}$, $\hat{p}^a_{\rm out}$) and antisqueezing ($\hat{x}^a_{\rm out}$, $\hat{p}^b_{\rm out}$).

The rotating-wave approximation in Eq. (7) requires the weak coupling $\omega_s > g_s$ and $|\Delta_o| + \omega_s \gg |\Delta_o| - \omega_s$, indicating $\omega_s \neq 0$, thus, forbids β becoming one. The Bogoliubov transformation also requires $\beta < 1$ which means the system cannot really approach the amplification threshold. Fortunately, as shown by the orange curve in Fig. 3 with $\beta = 0.95, 0.8$, the channel enhancement is already enormous when the system is close to the threshold, thus, we give it the name "near-amplification threshold enhancement." Note the constraint $\beta < 1$ is purely from the Bogoliubov framework. Practically, β can be any physical value and how to remove the corresponding squeezing-amplified noise is an interesting topic for the future.

A possible extension of the scheme is to further introduce two-photon drive on the optical mode and explore how the

half-matching condition develops. In the Bogoliubov picture, this could also strengthen the coupling strength. It is worth mentioning that as the coupling strength increases (larger than the mode loss), one might enter the strong-coupling regime where mode splitting will happen in the conversion spectrum [57]. In this case, the optimal transmissivity is not at $\omega = 0$ anymore (currently we assume the system is weakly coupled) and should be taken into account in future implementations.

Acknowledgments. We acknowledge support from the ARO (Grants No. W911NF-18-1-0020 and No. W911NF-18-1-0212), ARO MURI (Grants No. W911NF-16-1-0349 and No. W911NF-21-1-0325), AFOSR MURI (Grants No. FA9550-19-1-0399 and No. FA9550-21-1-0209), AFRL (Grant No. FA8649-21-P-0781), DOE Q-NEXT, NSF (Grants No. OMA-1936118, No. EEC-1941583, and No. OMA-2137642), NTT Research, and the Packard Foundation (Grant No. 2020-71479).

[1] A. Blais, A. L. Grimsmo, S. M. Girvin, and A. Wallraff, Circuit quantum electrodynamics, Rev. Mod. Phys. **93**, 025005 (2021).

[2] J. Yin, Y. Cao, Y.-H. Li, S.-K. Liao, L. Zhang, J.-G. Ren, W.-Q. Cai, W.-Y. Liu, B. Li, H. Dai *et al.*, Satellite-based entanglement distribution over 1200 kilometers, Science **356**, 1140 (2017).

[3] J. I. Cirac, P. Zoller, H. J. Kimble, and H. Mabuchi, Quantum State Transfer and Entanglement Distribution among Distant Nodes in a Quantum Network, Phys. Rev. Lett. **78**, 3221 (1997).

[4] H. J. Kimble, The quantum internet, Nature (London) **453**, 1023 (2008).

[5] R. W. Andrews, R. W. Peterson, T. P. Purdy, K. Cicak, R. W. Simmonds, C. A. Regal, and K. W. Lehnert, Bidirectional and efficient conversion between microwave and optical light, Nat. Phys. **10**, 321 (2014).

[6] A. Vainsencher, K. J. Satzinger, G. A. Peairs, and A. N. Cleland, Bi-directional conversion between microwave and optical frequencies in a piezoelectric optomechanical device, Appl. Phys. Lett. **109**, 033107 (2016).

[7] M. Mirhosseini, A. Sipahigil, M. Kalaee, and O. Painter, Superconducting qubit to optical photon transduction, Nature (London) **588**, 599 (2020).

[8] E. Zeuthen, A. Schliesser, A. S. Sørensen, and J. M. Taylor, Figures of merit for quantum transducers, Quantum Sci. Technol. **5**, 034009 (2020).

[9] C. Weedbrook, S. Pirandola, R. García-Patrón, N. J. Cerf, T. C. Ralph, J. H. Shapiro, and S. Lloyd, Gaussian quantum information, Rev. Mod. Phys. **84**, 621 (2012).

[10] C. A. Regal and K. W. Lehnert, From cavity electromechanics to cavity optomechanics, J. Phys.: Conf. Ser. **264**, 012025 (2011).

[11] J. Bochmann, A. Vainsencher, D. D. Awschalom, and A. N. Cleland, Nanomechanical coupling between microwave and optical photons, Nat. Phys. **9**, 712 (2013).

[12] J. M. Taylor, A. S. Sørensen, C. M. Marcus, and E. S. Polzik, Laser Cooling and Optical Detection of Excitations in a *LC* Electrical Circuit, Phys. Rev. Lett. **107**, 273601 (2011).

[13] S. Barzanjeh, D. Vitali, P. Tombesi, and G. J. Milburn, Entangling optical and microwave cavity modes by means of a nanomechanical resonator, Phys. Rev. A **84**, 042342 (2011).

[14] Y.-D. Wang and A. A. Clerk, Using Interference for High Fidelity Quantum State Transfer in Optomechanics, Phys. Rev. Lett. **108**, 153603 (2012).

[15] L. Tian and H. Wang, Optical wavelength conversion of quantum states with optomechanics, Phys. Rev. A **82**, 053806 (2010); L. Tian, Adiabatic State Conversion and Pulse Transmission in Optomechanical Systems, Phys. Rev. Lett. **108**, 153604 (2012); Optoelectromechanical transducer: Reversible conversion between microwave and optical photons, Ann. Phys. (N. Y.) **527**, 1 (2015).

[16] L. Midolo, A. Schliesser, and A. Fiore, Nano-opto-electro-mechanical systems, Nat. Nanotechnol. **13**, 11 (2018).

[17] T. Bagci, A. Simonsen, S. Schmid, L. G. Villanueva, E. Zeuthen, J. Appel, J. M. Taylor, A. Sørensen, K. Usami, A. Schliesser, and E. S. Polzik, Optical detection of radio waves through a nanomechanical transducer, Nature (London) **507**, 81 (2014).

[18] M. Winger, T. D. Blasius, T. P. M. Alegre, A. H. Safavi-Naeini, S. Meenehan, J. Cohen, S. Stobbe, and O. Painter, A chip-scale integrated cavity-electro-optomechanics platform, Opt. Express **19**, 24905 (2011).

[19] A. Pitanti, J. M. Fink, A. H. Safavi-Naeini, J. T. Hill, C. U. Lei, A. Tredicucci, and O. Painter, Strong opto-electro-mechanical coupling in a silicon photonic crystal cavity, Opt. Express **23**, 3196 (2015).

[20] M. Tsang, Cavity quantum electro-optics, Phys. Rev. A **81**, 063837 (2010); Cavity quantum electro-optics. II. input-output relations between traveling optical and microwave fields, **84**, 043845 (2011).

[21] C. Javerzac-Galy, K. Plekhanov, N. R. Bernier, L. D. Toth, A. K. Feofanov, and T. J. Kippenberg, On-chip microwave-to-optical quantum coherent converter based on a superconducting resonator coupled to an electro-optic microresonator, Phys. Rev. A **94**, 053815 (2016).

[22] L. Fan, C.-L. Zou, R. Cheng, X. Guo, X. Han, Z. Gong, S. Wang, and H. X. Tang, Superconducting cavity electro-optics: a platform for coherent photon conversion between superconducting and photonic circuits, Sci. Adv. **4**, eaar4994 (2018).

[23] W. Fu, M. Xu, X. Liu, C.-L. Zou, C. Zhong, X. Han, M. Shen, Y. Xu, R. Cheng, S. Wang, L. Jiang, and H. X. Tang, Cavity electro-optic circuit for microwave-to-optical conversion in the quantum ground state, Phys. Rev. A **103**, 053504 (2021).

[24] R. Hisatomi, A. Osada, Y. Tabuchi, T. Ishikawa, A. Noguchi, R. Yamazaki, K. Usami, and Y. Nakamura, Bidirectional conversion between microwave and light via ferromagnetic magnons, Phys. Rev. B **93**, 174427 (2016).

[25] N. Zhu, X. Zhang, X. Han, C.-L. Zou, C. Zhong, C.-H. Wang, L. Jiang, and H. X. Tang, Waveguide cavity optomagnonics for microwave-to-optics conversion, Optica **7**, 1291 (2020).

[26] J. Han, T. Vogt, C. Gross, D. Jaksch, M. Kiffner, and W. Li, Coherent Microwave-to-Optical Conversion via Six-Wave Mixing in Rydberg Atoms, Phys. Rev. Lett. **120**, 093201 (2018).

[27] A. H. Safavi-Naeini and O. Painter, Proposal for an optomechanical traveling wave phonon–photon translator, New J. Phys. **13**, 013017 (2011).

[28] C. H. Bennett, D. P. DiVincenzo, and J. A. Smolin, Capacities of Quantum Erasure Channels, Phys. Rev. Lett. **78**, 3217 (1997).

[29] R. García-Patrón, S. Pirandola, S. Lloyd, and J. H. Shapiro, Reverse Coherent Information, Phys. Rev. Lett. **102**, 210501 (2009).

[30] S. Barzanjeh, M. Abdi, G. J. Milburn, P. Tombesi, and D. Vitali, Reversible Optical-to-Microwave Quantum Interface, Phys. Rev. Lett. **109**, 130503 (2012).

[31] C. Zhong, Z. Wang, C. Zou, M. Zhang, X. Han, W. Fu, M. Xu, S. Shankar, M. H. Devoret, H. X. Tang, and L. Jiang, Proposal for Heralded Generation and Detection of Entangled Microwave–Optical-Photon Pairs, Phys. Rev. Lett. **124**, 010511 (2020).

[32] A. Rueda, W. Hease, S. Barzanjeh, and J. M. Fink, Electro-optic entanglement source for microwave to telecom quantum state transfer, npj Quantum Inf. **5**, 108 (2019).

[33] C. Zhong, X. Han, and L. Jiang, Quantum transduction with microwave and optical entanglement, arXiv:2202.04601.

[34] J. Wu, C. Cui, L. Fan, and Q. Zhuang, Deterministic Microwave-Optical Transduction Based on Quantum Teleportation, Phys. Rev. Appl. **16**, 064044 (2021).

[35] A. P. Higginbotham, P. Burns, M. Urmey, R. Peterson, N. Kampel, B. Brubaker, G. Smith, K. Lehnert, and C. Regal, Harnessing electro-optic correlations in an efficient mechanical converter, Nat. Phys. **14**, 1038 (2018).

[36] M. Zhang, C.-L. Zou, and L. Jiang, Quantum Transduction with Adaptive Control, Phys. Rev. Lett. **120**, 020502 (2018).

[37] H.-K. Lau and A. A. Clerk, High-fidelity bosonic quantum state transfer using imperfect transducers and interference, npj Quantum Inf. **5**, 31 (2019).

[38] R. Sahu, W. Hease, A. Rueda, G. Arnold, L. Qiu, and J. M. Fink, Quantum-enabled operation of a microwave-optical interface, Nat. Commun. **13**, 1276 (2022).

[39] M. M. Wilde, *Quantum Information Theory* (Cambridge University Press, Cambridge, UK, 2013).

[40] H.-K. Lau and A. A. Clerk, Ground-State Cooling and High-Fidelity Quantum Transduction via Parametrically Driven Bad-Cavity Optomechanics, Phys. Rev. Lett. **124**, 103602 (2020).

[41] S. Huang and G. S. Agarwal, Enhancement of cavity cooling of a micromechanical mirror using parametric interactions, Phys. Rev. A **79**, 013821 (2009).

[42] W. Qin, A. Miranowicz, P.-B. Li, X.-Y. Lü, J. Q. You, and F. Nori, Exponentially Enhanced Light-Matter Interaction, Cooperativities, and Steady-State Entanglement Using Parametric Amplification, Phys. Rev. Lett. **120**, 093601 (2018).

[43] X.-Y. Lü, Y. Wu, J. R. Johansson, H. Jing, J. Zhang, and F. Nori, Squeezed Optomechanics with Phase-Matched Amplification and Dissipation, Phys. Rev. Lett. **114**, 093602 (2015).

[44] C. Leroux, L. C. G. Govia, and A. A. Clerk, Enhancing Cavity Quantum Electrodynamics via Antisqueezing: Synthetic Ultrastrong Coupling, Phys. Rev. Lett. **120**, 093602 (2018).

[45] V. Peano, H. G. L. Schwefel, C. Marquardt, and F. Marquardt, Intracavity Squeezing Can Enhance Quantum-Limited Optomechanical Position Detection through Deamplification, Phys. Rev. Lett. **115**, 243603 (2015).

[46] H. Chen, M. Vives, and M. Metcalf, Parametric amplification of an optomechanical quantum interconnect, arXiv:2202.12291.

[47] L. Tang, J. Tang, M. Chen, F. Nori, M. Xiao, and K. Xia, Quantum Squeezing Induced Optical Nonreciprocity, Phys. Rev. Lett. **128**, 083604 (2022).

[48] M.-A. Lemonde, N. Didier, and A. A. Clerk, Enhanced nonlinear interactions in quantum optomechanics via mechanical amplification, Nat. Commun. **7**, 11338 (2016).

[49] See Supplemental Material at http://link.aps.org/supplemental/10.1103/PhysRevResearch.4.L042013 for the brief introduction of the bosonic quantum channel and quantum capacity, the EO-induced transduction channel, Euler decomposition, the derivation for Bogoliubov transformation, and the discussion of the squeezing-noise elimination technique.

[50] The extraction ratio is defined as signal coupling rate to the total loss rate, e.g., $\zeta_{\rm o} \equiv \kappa_{\rm o,c}/\kappa_{\rm o}$, where $\kappa_{\rm o,c}$ is the signal coupling rate, and $\kappa_{\rm o,i} = \kappa_{\rm o} - \kappa_{\rm o,c}$ is called the intrinsic loss rate.

[51] M. Malnou, D. A. Palken, L. R. Vale, G. C. Hilton, and K. W. Lehnert, Optimal Operation of a Josephson Parametric Amplifier for Vacuum Squeezing, Phys. Rev. Appl. **9**, 044023 (2018).

[52] J. Eisert and M. M. Wolf, Gaussian quantum channels, arXiv:quant-ph/0505151.

[53] M. A. De Gosson, *Symplectic Geometry and Quantum Mechanics* (Springer, Berlin, 2006), Vol. 166.

[54] M. O. Scully, M. S. Zubairy *et al.*, *Quantum Optics* (Cambridge University Press, Cambridge, UK, 1997).

[55] G. S. Agarwal, *Quantum Optics* (Cambridge University Press, Cambridge, UK, 2012).

[56] M. Aspelmeyer, T. J. Kippenberg, and F. Marquardt, Cavity optomechanics, Rev. Mod. Phys. **86**, 1391 (2014).

[57] C. Zhong, X. Han, H. X. Tang, and L. Jiang, Entanglement of microwave-optical modes in a strongly coupled electro-optomechanical system, Phys. Rev. A **101**, 032345 (2020).